SRF MULTILAYER STRUCTURES BASED ON NBTIN *

A.-M. Valente-Feliciano[#], H. L. Phillips, C. E. Reece, and J. K. Spradlin
Thomas Jefferson National Accelerator Facility, Newport News, VA 23606, U.S.A.
K. Seo, Norfolk State University, VA 60439, U.S.A.
A. D. Batchelor, F. Stevie, North Carolina State University, Raleigh, NC 27695, U.S.A.
R. A. Lukaszew, College William & Mary, VA 23185, U.S.A.

Abstract

For the past three decades, bulk niobium has been the material of choice for SRF cavities applications. In recent years, RF cavity performance has approached the theoretical limit for bulk niobium. To further improve RF cavity performance for future accelerator projects an interesting alternative has been recently proposed by A. Gurevich, a Superconductor-Insulator-Superconductor multilayer. This approach uses the benefit of the higher critical field H_{c2} of higher-Tc superconductors without being limited with their lower H_{c1} thereby avoiding early flux penetration.

JLab is pursuing this approach with the development of multilayer structures based on NbTiN via magnetron sputtering and High Power Impulse Magnetron Sputtering (HiPIMS). Insulators such as, AlN, Al_2O_3 and MgO are being investigated as candidates for the insulator layers.

This paper presents the preliminary results on the characteristics of NbTiN and insulator layers and a first attempt of a NbTiN-based multilayer structure on bulk Nb and thick Nb films.

SIS MULTILAYER APPROACH FOR SRF CAVITIES

A few years ago, a concept was proposed by A. Gurevich [1] which would allow taking advantage of high-Tc superconductors without being penalized by their lower Hc₁. The idea is to coat superconducting radio-frequency (SRF) cavities with alternating superconducting and insulating layers (SIS structures) with a thickness d smaller than the penetration depth λ (figure 1). If the superconducting film is deposited with a thickness d $\ll\lambda$, the Meissner state can be retained at a magnetic field much higher than the bulk H_{c1}. The strong increase of H_{c1} in films allows utilization of RF fields higher than the critical field H_c of Nb but lower than those at which the flux penetration at grain boundaries may create a problem. The thin higher-Tc layers provide magnetic screening of the bulk superconducting cavity preventing vortex penetration. The BCS resistance is also strongly reduced because the superconducting materials used have higher gap Δ (Nb_3Sn, NbTiN …) than Nb. With such structures, Q-values at 4.2K could be increased two orders of magnitude above Nb values.

If a 50nm Nb_3Sn layer is coated on a bulk Nb cavity with an insulating interlayer and if the Nb cavity can sustain fields up to 150mT, this structure could potentially sustain external magnetic fields of about 320mT and therefore reach accelerating gradients without precedent.
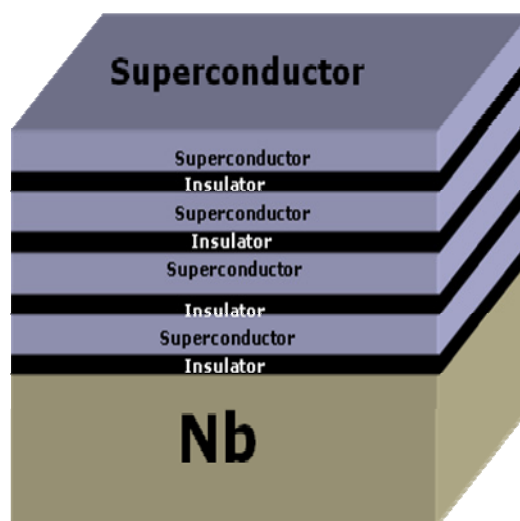

Figure 1: The SIS multilayer approach.

CANDIDATE MATERIALS

Superconductor: NbTiN

Although A15 compounds such as Nb_3Sn have a higher T_c, the Nb B1 compounds are less sensitive to radiation damage and crystalline disorder.

B1 compounds have a NaCl structure (figure 2) where metallic atoms A form a face centred cubic (fcc) lattice and non-metallic atoms B occupy all the octahedral interstices. These compounds are characterized by the fact that they always have a certain amount of vacancies, usually distributed randomly throughout the lattice [2]. The superconducting properties of B1 compounds are very sensitive to deviation from stoichiometric composition

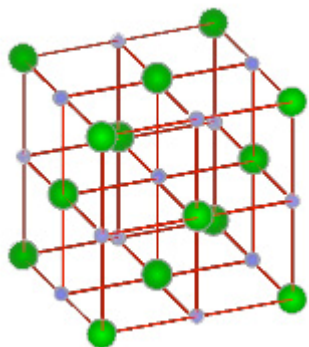NbN and NbTiN are the B1-compounds with the highest critical temperature, respectively 17.3K and 17.8K.

Figure 2: NaCl (B1) structure.

The phase diagram of the binary system Nb-N up to N/Nb=1 includes many different phases [3, 4], characterized by different Tc [5]. The B1-NbN superconducting phase of interest *(cubic δ-phase, a=4.388Å)* is only thermodynamically metastable at room temperature. Tc is very sensitive to the nitrogen (N) stoichiometry and NbN suffers from a high resistivity due to the presence of both metallic and gaseous vacancies randomly distributed in both sub-lattices, in amount of 1.3% respectively. The equi-atomic composition is $Nb_{0.987}N_{0.987}$ [6].

The ternary nitride NbTiN presents all the advantages of NbN and exhibits increased metallic electrical conduction properties with higher titanium (Ti) percentage. Ti is a good nitrogen getter, so the higher the Ti composition, the lower the number of vacancies. In contrast with NbN, the B1-TiN phase is stable at room temperature (Tc=5K, a=4.24Å). The two nitride phases are completely miscible   resulting in a superconducting ternary NbTiN cubic phase which remains thermodynamically stable at room temperature [7]. T_c is slightly higher for NbTiN but as for NbN, N stoichiometry is critical to obtaining the right superconducting phase.

Some of the common techniques used to produce NbTiN are reactive magnetron sputtering [8] and high impulse magnetron sputtering [9].

Insulator: AlN

AlN is an insulator that can be grown with a wurtzite (hexagonal close-packed, a=3.11Å, c=4.98Å) or sphalerite (B1 cubic, a= 4.08 Å) structure (figure 3).

AlN has been found to enhance the properties (T_c) of NbN and NbTiN, in particular for very thin films [10]. Its thermal conductivity is large ($3.19W/cm^2$ at 300 K), comparable with Cu ($4.01W/cm^2$).

AlN films have been extensively used for their dielectric and piezo-electric properties for multilayer terra-hertz (THz) mixers and surface acoustic wave sensors.
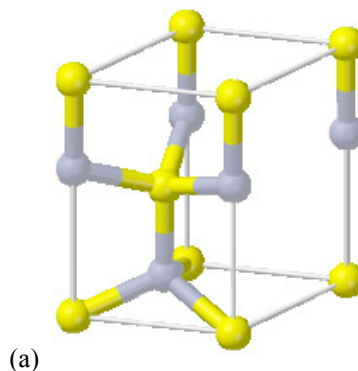
(a)
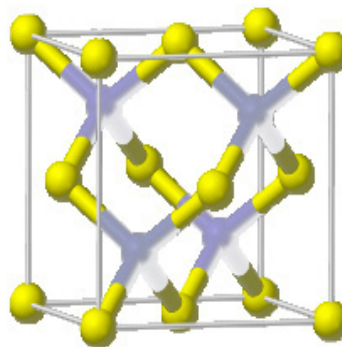
(b)

Figure 3: Wurtzite (a) and sphalerite (b) structures.

EXPERIMENTAL METHOD

This study uses an ultra-high vacuum (UHV) multi-technique deposition system tailored to in-situ multilayer depositions. The system (figure 4) is equipped with three RF/DC magnetron heads for 50 mm targets and a RF/DC Ion source producing a 50mm beam with Ar or Kr. A self-sputter magnetron for implementation of HiPIMS is available and will be added to the system in the near future. A set of thickness monitors allows for thickness control of the deposited layers of different materials. Several injection lines are available on the main chamber for the injection of the sputtering working gas (Ar and Kr) and N_2 and O_2 used for reactive sputtering.

This combination allows the implementation of DC magnetron sputtering for the deposition of metallic films or compounds. NbN, NbTiN compounds, as well as dielectric films can be coated via DC or RF reactive sputtering. RF magnetron sputtering is commonly used

for the deposition of insulator layers like Al_2O_3 and MgO.

The implementation of HiPIMS will allow the use energetic ions to modify film density, stress, texture, grain size, structure of the interface and other related properties.

The main chamber is pumped with a cryopump CTI Cryo-Torr 8 (1500 l/s) through a VAT throttle gate valve. The base pressure for the main chamber is 1×10^{-9} Torr. During deposition, to allow a better control of the working gas pressure, the throttle valve aperture can be varied to adjust the pumping speed. The system is also equipped with a non-evaporable getter (NEG) chamber to improve hydrogen pumping during the deposition process. A strip of ST707 mounted on a cylindrical support can provide pumping speeds up to 2000l/s for H_2 and CO. An, internal UV desorption system is used during pump down to desorb water from the chamber walls. Plasma cleaning can also be used to further improve the vacuum quality.

The vacuum is monitored by the combination of a convectron gauge, an UHV ion gauge in each chamber and a Residual Gas Analyser (RGA) that can be used with differential pumping allowing the analysis of the gas composition in the vacuum system during deposition. A high-pressure ionization gauge is used in the main chamber to measure the working gas pressure during deposition.
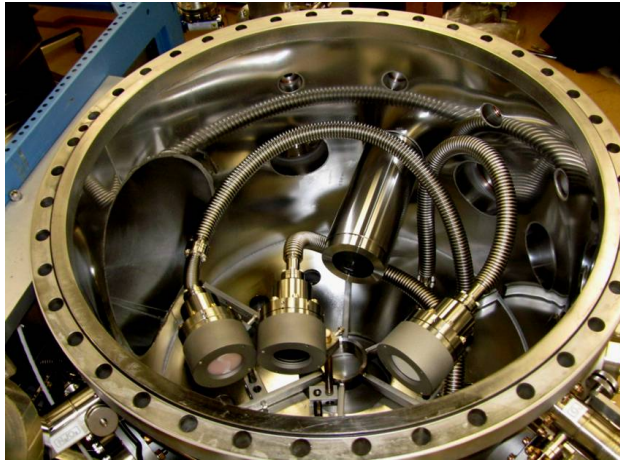

Figure 4: Setup in the UHV multi-technique deposition system main chamber.

Multiple sample holders are available on the main chamber to allow the simultaneous deposition of witness samples to probe the quality and properties of the individual layers and allow the variation of deposition parameters during the same deposition run. All sample stages can be heated up to 800°C and are equipped with shutters to allow the deposition in the same run of multiple sets of samples with different parameters, ensuring directly comparable environmental conditions.

Nucleation studies for each type of layer are performed in parallel with the William & Mary UHV system equipped with RHEED. In addition to the standard set of measurements, i.e. surface and material characterization coupled to cryogenic and RF measurements with the SIC cavity, a method is being developed to observe the onset of flux penetration in the produced SIS multilayer structures.

NBTIN FILMS

NbTiN were grown on various substrates at 600°C by DC reactive sputtering with targets of different Nb/Ti weight ratios: 55%/45%, 70%/30% and 80%/20%. The best transition temperatures were achieved with a $Nb_{80wt.\%}/Ti_{20wt.\%}$ target. Table 1 summarizes the coating parameters and properties for the best NbTiN films.

Table 1: Coating parameters for the best NbTiN films

	NbTiN
N_2/Ar	0.23
Total Pressure [Torr]	2×10^{-3}
Sputtering Power [W]	300
Deposition rate [nm/min]	18

We investigated the substrate dependence of the crystallographic structures of NbTiN films by XRD analysis. The films deposited on crystalline substrate exhibit relatively good structure. Figure 5 shows the XRD patterns for 90nm thick NbTiN films on (a) single-crystal MgO(100), (b) Al_2O_3(11-20), and (c) w-AlN(0001)/Al_2O_3(11-20) substrates. The NbTiN film grown on MgO shows clear (200) and (400) peaks, indicating epitaxial growth on the MgO (100) substrate, with a lattice parameter of 4.36Å. The film grown on sapphire exhibits epitaxial growth with NbTiN (111) and (222) reflections. For the film grown on an epitaxial AlN layer on sapphire, the θ-2θ scan reveals the expected w-AlN (0001) reflection along with NbTiN (222) and (400).

T_c measurements were conducted via the four-point probe method. The multi-sample measurement setup uses a calibrated CERNOX thermometer with 50mK sensitivity. However, calibration refinements of the system are under way for error determination due to sample position variability.

The results are reported in tables 2 and 3 for films, respectively 90 nm and 175 nm thick, deposited on the various substrates mentioned above. The best T_c was obtained for films deposited on MgO, 16.2K for a thickness of about 600 nm. We did not yet observe the enhancement of T_c reported in literature for NbTiN deposited on AlN.
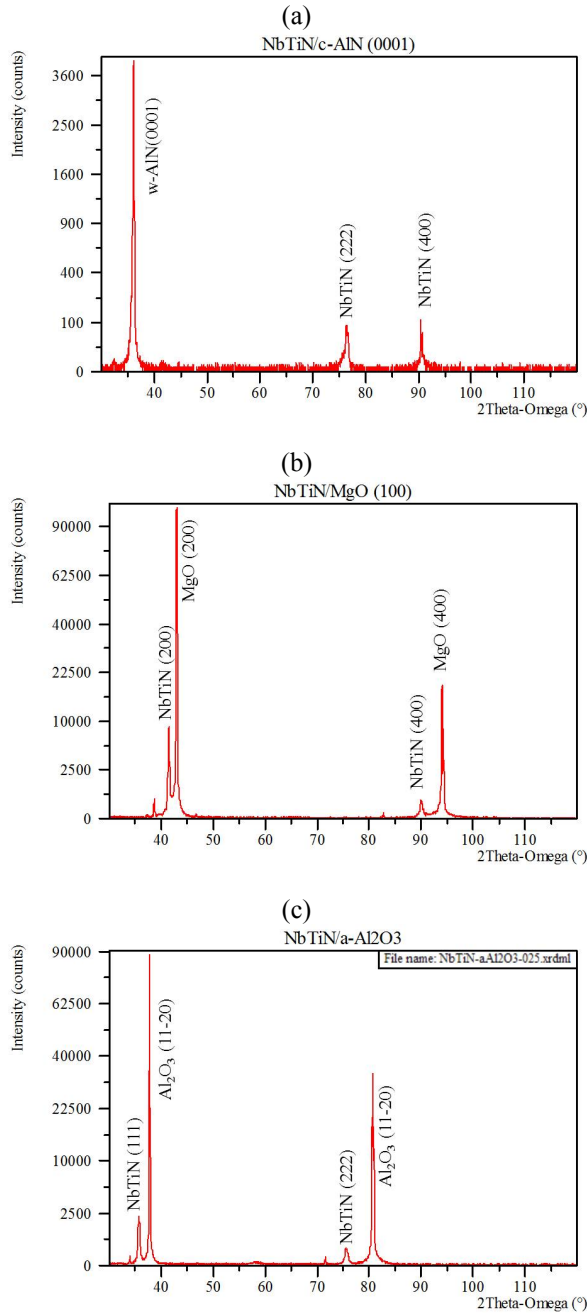
(a)

NbTiN/c-AlN (0001)

(b)

NbTiN/MgO (100)

(c)

NbTiN/a-Al2O3

Figure 5: XRD Bragg-Brentano (θ−2θ) spectra for 90 nm thick NbTiN coated simultaneously on (a) w-AlN (0001)/Al_2O_3 (11-20), (b) MgO (100) and (c) Al_2O_3 (11-20).

Table 2: Transition temperatures and width for 175 and 90 nm thick NbTiN films on different substrates.

	175 nm		90 nm	
	T_c[K]	ΔT_c[K]	T_c[K]	ΔT_c[K]
AlN(0001)/Al_2O_3 (11-20)	14.69	0.23	14.19	0.09
AlN ceramic	13.97	0.87	12.91	0.26
MgO (100)	16.14	0.48	16.10	0.65
Al_2O_3(11-20)	15.33	0.45	15.43	0.45

AᴌN FILMS

Reactive sputtering of an elemental Al (99.999%) target was carried out with different N_2/Ar ratios and power values. The MgO (100) substrates were heated to 600°C for 24 hours. They were maintained at the same temperature during coating and for 4 hours after, for annealing. The AlN layers became fully transparent for N_2/Ar ratios of about 33%. The corresponding deposition conditions are reported in table 2.

Table 3: Coating parameters for AlN

	AlN
N_2/Ar	0.33
Total Pressure [Torr]	$2x10^{-3}$
Sputtering Power [W]	100
Deposition rate [nm/min]	15

The film was examined by θ-2θ x-ray diffraction with Cu$K\alpha$ radiation. Figure 6 shows a θ-2θ scan of an AlN film of about 10 nm in thickness. The scan shows the expected MgO (200) and (400). The only reflections observed for AlN are at 38.54° and 82.70°, corresponding to B1-AlN (111) and (222) respectively. The lattice parameter a_0 is 4.04Å.
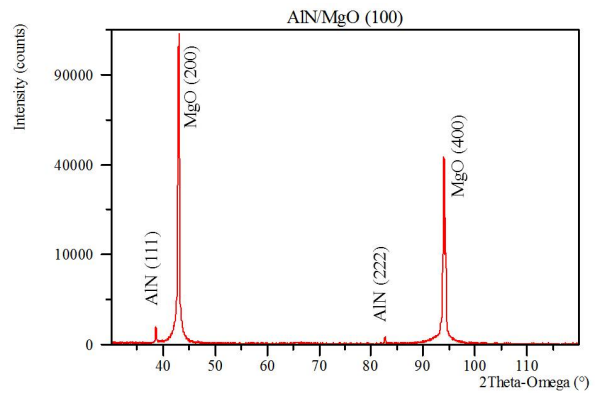
AlN/MgO (100)

Figure 6: XRD Bragg-Brentano spectrum for AlN coated on MgO (100).

Additional analyses such as stoichiometry, dielectric constant measurements are under way.

NBTIN/ALN STRUCTURES

Preliminary SIS structures have been coated (table 4) at 600°C in-situ on bulk Nb and Nb/Cu substrates. The substrates were heated at 600°C for 12 hours

Table 4: Coating conditions and properties for NbTiN/AlN structures

	AlN	NbTiN
N_2/Ar	0.33	0.23
Total Pressure [Torr]	2×10^{-3}	2×10^{-3}
Sputtering Power [W]	100	300
Deposition rate [nm/min]	~5	~18
Thickness [nm]	10	100
T_c [K]	N/A	14

Cross-section samples were cut by FIB (focused ion beam) to be observed by TEM. The TEM cross section (figure 7) reveals some non-uniformity at the interface of the NbTiN and AlN films. This could be due to the miscibility of Nb and Al at high temperatures [11]. The

A-M #@_001.tif
A-M #2
Print Mag: 236000x @ 7.0 in
16:22 07/19/11
TEM Mode: Imaging

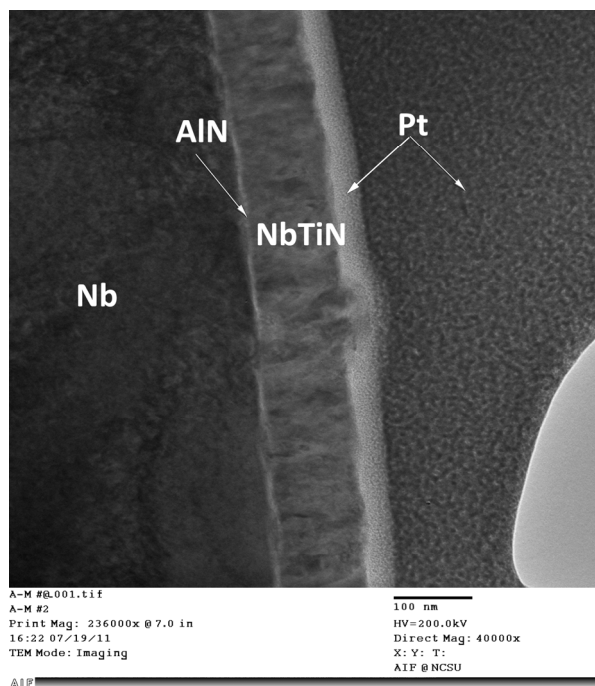100 nm
HV=200.0kV
Direct Mag: 40000x
X: Y: T:
AIF @ NCSU

Figure 7: TEM image of a FIB cut NbTiN/AlN/Nb/Cu structure. Due to magnification, only the NbTiN/AlN/Nb can be seen on the micrograph.

interface needs to be analyzed by electron desorption spectroscopy (EDS) to verify this hypothesis. Further analysis is underway. Additional structures will also be coated at lower temperature as well as with MgO for the insulator layer.

Once the structure is optimized, 50mm disks will be coated and measured in setups specifically designed for SIS multilayers where RF fields parallel to the structure surface can be applied [12,13].

CONCLUSION

- JLab in collaboration with surrounding universities (College William & Mary, Old Dominion University, and Norfolk State University) is pursuing the opportunity to create SIS multilayer structures following the concept proposed by A. Gurevich for overcoming the fundamental bulk material limitation, H_{c1}. This has the potential to create viable superconducting RF cavity surfaces that will reduce the cost framework of SRF accelerators, reach higher gradients, and allow operation of SRF structures at 4K.
- Good quality NbTiN and AlN films have been produced by DC reactive sputtering. The first multilayer structures have been deposited and are under analysis.
- HiPIMS will be implemented in the near future as an energetic condensation deposition technique. This will allow production of films, possibly at lower temperatures, with higher density and crystalline quality [9, 14, 15].

AKNOWLEDGEMENT

REFERENCES

[1] A. Gurevich, Appl. Phys. Lett. 88, 012511 (2006).
[2] S. V. Vonsovsky, Yu. A. Izyumov, E. Z. Kumaev, "Superconductivity of transition metals, their alloys and compounds", Springer-Verlag (1982).
[3] G. Brauer, J. Less-Common Metals 2 (1960) 131.
[4] R.W. Guard, J.W. Savage and D.G. Swarthout, Trans. Metall. Soc. ATME 239 (1967) 643.
[5] L. Toth, Transition Metal Carbides and Nitrides (Academic Press, New York, 1971), chap. 7.
[6] V. Palmieri, 10th Workshop on RF Super-conductivity Proceedings, Tsukuba 2001 (Noguchi) 162-169.
[7] C. Benvenuti et al. Nucl. Instrum. Methods B 124 (1997) 106-111.

[8]   A. Nigro et al., Adv. Cryog. Eng. 34, 813 (1988).

[9]   Y.P. Purandare, A.P. Ehiasarian, and P. Eh. Hovsepian, J. Vac. Sci. Technol. A 26(2) 288, (2008).

[10] T. Shiino et al., Supercond. Sci. Technol. 23 045004 (2010).

[11] S. Yoshimori, Physica C 305,281–284(1998)

[12] C. Antoine et al. TUIOA03.

[13] D. Bowring, PhD thesis, Uni. Virginia/JLAB (2011).

[14] A M. Samuelsson et al., Surface and Coatings Technology 205 (2), 591-596 (2010).

[15] Guillaumot, Vacuum 85 (2), 120-125 (2010).